



# The effect of particle acidity on secondary organic aerosol formation from $\alpha$ -pinene photooxidation under atmospherically relevant conditions

Yuemei Han, Craig A. Stroud, John Liggio, and Shao-Meng Li

Air Quality Research Division, Atmospheric Science and Technology Directorate, Environment and Climate Change  
5 Canada, Toronto, ON, M3H 5T4, Canada

*Correspondence to:* Craig A. Stroud (craig.stroud@canada.ca) and Yuemei Han (yuemeihan@hotmail.com)

**Abstract.** Secondary organic aerosol (SOA) formation from OH-initiated photooxidation of  $\alpha$ -pinene has been investigated in a photochemical reaction chamber under varied particle acidity levels. The effect of particle acidity on SOA yield and chemical composition was examined under high- and low- $\text{NO}_x$  conditions. The SOA yield (4.0%–7.3%) increased nearly 10 linearly with the increase in particle acidity under high- $\text{NO}_x$  conditions. In contrast, the SOA yield (27.9%–35.6%) was substantially higher under low- $\text{NO}_x$  conditions, but its dependency on particle acidity was insignificant. A relatively strong increase in SOA yield (up to 220%) was observed in the first hour of  $\alpha$ -pinene photooxidation under high- $\text{NO}_x$  conditions, suggesting that SOA formation was more effective for early  $\alpha$ -pinene oxidation products in the presence of fresh acidic particles. The SOA yield decreased gradually with the increase in organic mass under high- $\text{NO}_x$  conditions, which is likely 15 due to the inaccessibility of the acidity over time with the coating of  $\alpha$ -pinene SOA. The formation of later-generation SOA was enhanced by particle acidity even under low- $\text{NO}_x$  conditions when introducing acidic seed particles after  $\alpha$ -pinene photooxidation. The fraction of oxygen-containing organic fragments ( $\text{C}_x\text{H}_y\text{O}_1^+$  33–35% and  $\text{C}_x\text{H}_y\text{O}_2^+$  16–17%) in the total organics and the O/C ratio (0.49–0.54) of  $\alpha$ -pinene SOA were lower under high- $\text{NO}_x$  conditions than those under low- $\text{NO}_x$  20 conditions (39–40%, 17–19%, and 0.60–0.62), suggesting that  $\alpha$ -pinene SOA was less oxygenated in the studied high- $\text{NO}_x$  conditions. The fraction of nitrogen-containing organic fragments ( $\text{C}_x\text{H}_y\text{N}_z^+$  and  $\text{C}_x\text{H}_y\text{O}_z\text{N}_p^+$ ) in the total organics was enhanced with the increases in particle acidity under high- $\text{NO}_x$  conditions, indicating that organic nitrates may be formed 25 heterogeneously through a mechanism catalyzed by particle acidity. The results of this study suggest that inorganic acidity have a significant role to play in determining various organic aerosol chemical properties such as oxidation state, mass yields, and organic nitrate content. It is also an important parameter in the modeling of SOA, which is further dependent on the time scale of SOA formation. Additional research is required to understand the complex physical and chemical interactions facilitated by aerosol acidity.

## 1 Introduction

Secondary organic aerosols (SOA) formed by oxidation of biogenic and anthropogenic volatile organic compounds (VOCs) comprise a substantial portion of submicron aerosol particles in the atmosphere (Kanakidou et al., 2005; Zhang et



30 al., 2007a). Understanding the physical and chemical properties associated with SOA formation and transformation is important to adequately assess aerosol impacts on climate and human health (Hallquist et al., 2009). The effect of aerosol acidity on SOA formation is one of the scientific questions currently under open debate, as results obtained from both laboratory and field studies tend to be inconsistent. Acid-catalyzed heterogeneous reactions such as hydration, hemiacetal/acetal formation, polymerization, and aldol condensation have been proposed to form SOA (Jang et al., 2002).  
35 The presence of acidic aerosol particles has been shown to enhance the reactive uptake of particle phase organics and increase SOA yields due to acid-catalyzed reactions (i.e., Garland et al., 2006; Jang et al., 2004; Liggio and Li, 2006; Northcross and Jang, 2007). However, other studies have suggested that those reactions may be thermodynamically or kinetically unfavorable and are possibly insignificant in the real atmosphere (Barsanti and Pankow, 2004; Casale et al., 2007; Kroll et al., 2005; Li et al., 2008). Furthermore, the enhanced formation of SOA, organic sulfates, and epoxide compounds  
40 has been reported in ambient environments with an abundance of acidic aerosol particles (Hawkins et al., 2010; Lin et al., 2012; Rengarajan et al., 2011; Zhang et al., 2012; Zhou et al., 2012), which is contrary to other field studies showing no apparent evidence of acid-catalyzed SOA formation (Peltier et al., 2007; Takahama et al., 2006; Tanner et al., 2009; Zhang et al., 2007b). The dependence of SOA formation on aerosol acidity has not been considered in most atmospheric chemistry models thus far due to the large uncertainties associated with its quantification.

45 A number of laboratory studies have investigated the effect of particle acidity on SOA formation from oxidation of various precursor hydrocarbons such as isoprene, terpenes, toluene, m-xylene, and 1, 3-butadiene (e.g., Kristensen et al., 2014; Lewandowski et al., 2015; Ng et al., 2007a; Offenberg et al., 2009; Song et al., 2013; Surratt et al., 2007b).  $\alpha$ -Pinene is the most abundant biogenic monoterpene emitted from terrestrial vegetation (Guenther et al., 2012). The oxidation of  $\alpha$ -pinene by hydroxyl radicals (OH), ozone (O<sub>3</sub>), and nitrate radicals produces a variety of multifunctional organic compounds  
50 such as carboxylic acids, carbonyls, peroxides, epoxides, alcohols, and organic nitrates (Yasmeen et al., 2012). Despite the efforts of previous laboratory studies, large discrepancies among experiments remain with respect to the effect of aerosol acidity on SOA formation from individual hydrocarbons. In particular, the magnitude of the acidic effect on SOA yields for  $\alpha$ -pinene has been found to vary significantly. For instance, a nearly 40% increase in organic carbon (OC) was observed for the ozonolysis of  $\alpha$ -pinene in the presence of acidic seed particles without NO<sub>x</sub>, and aerosol acidity played an important role  
55 in the formation of high molecular weight organic molecules in particles (Iinuma et al., 2004). Enhanced aerosol acidity led to the formation of sulfate esters that contributed to a large fraction of SOA mass from photooxidation of  $\alpha$ -pinene under high-NO<sub>x</sub> conditions (Surratt et al., 2007a, 2008). A linear increase of 0.04% per nmol H<sup>+</sup> m<sup>-3</sup> in OC mass was reported from the photooxidation of  $\alpha$ -pinene with NO<sub>x</sub>, and this effect was independent of initial hydrocarbon concentration or the generated organic mass (Offenberg et al., 2009). In contrast, Eddingsaas et al. (2012) reported a relatively small increase of  
60 SOA yield (approximately 22%) for OH photooxidation of  $\alpha$ -pinene under high-NO<sub>x</sub> conditions, and no effect of aerosol acidity on SOA yield under low-NO<sub>x</sub> conditions. Kristensen et al. (2014) similarly found that the increase of aerosol acidity has a negligible effect on SOA formation from ozonolysis of  $\alpha$ -pinene under low-NO<sub>x</sub> conditions.



The large discrepancy regarding the previously reported acidity effect on  $\alpha$ -pinene SOA is most likely attributed to the varied experimental parameters such as particle acidity, initial hydrocarbon concentration, oxidant type and level,  $\text{NO}_x$  level, 65 temperature, and relative humidity (RH). Most previous studies were conducted with different acidity levels, and therefore a quantitative comparison of the acidity effect among various studies is problematic. Laboratory studies were usually performed with relatively high loading of hydrocarbons (e.g., from tens of ppb to several ppm level), which would result in higher yield and lower oxidation state of laboratory SOA compared to ambient SOA (Ng et al., 2010; Odum Jay et al., 1996; Pfaffenberger et al., 2013; Shilling et al., 2009). In addition, the presence of  $\text{NO}_x$  during  $\alpha$ -pinene oxidation may change the 70 reaction chemistry and lead to different oxidation products by introducing relatively volatile nitrogen-containing organic species, and hence decrease  $\alpha$ -pinene SOA yields (Eddingsaas et al., 2012; Ng et al., 2007a). Moreover, temperature is an important factor in SOA formation; higher SOA yields may be obtained at lower temperature (Saathoff et al., 2009; Takekawa et al., 2003). RH is another important factor, the decrease of which may lead to an increase in  $\alpha$ -pinene SOA 75 yields (Jonsson et al., 2006). However, many previous studies have been performed at very low RH (e.g., less than 10%) or even dry conditions. As a result of the above issues, it is highly important for laboratory studies to investigate the acidity effect on SOA formation under more realistic conditions approaching those of the ambient atmosphere. This would facilitate an accurate parameterization of the acidity effect for incorporation into air quality models.

This study aims to improve our current understanding of the effect of particle acidity on SOA formation from OH-initiated photooxidation of  $\alpha$ -pinene under conditions of relatively low  $\alpha$ -pinene loadings and moderate RH, which are more 80 representative of the ambient atmosphere. The dependence of  $\alpha$ -pinene SOA yield on particle acidity is characterized under high- and low- $\text{NO}_x$  conditions. The changes in the chemical composition of  $\alpha$ -pinene SOA with particle acidity and  $\text{NO}_x$  level are also examined. Finally, the potential significance of aerosol acidity in the formation of organic nitrates under high- $\text{NO}_x$  conditions is discussed.

## 2 Experimental methods

85 Photooxidation experiments were performed in a 2 m<sup>3</sup> Teflon chamber (Whelch Fluorocarbon) enclosed in an aluminum support (Liggio and Li, 2006; Liggio et al., 2005). Twelve black light lamps (model F32T8/350BL, Sylvania) were used as the irradiation source with intensity peaking at approximately 350 nm. The chamber was flushed by zero air with the lamps turned on for more than 20 hours before each experiment to avoid contamination from previous experiments. Hydrogen peroxide (H<sub>2</sub>O<sub>2</sub>) vapor was introduced into the chamber to produce OH radicals during the first 6 hours of flushing. 90 Temperature and RH inside the chamber were monitored continually using a temperature and humidity probe (model HMP 60, Vaisala). Temperature was not controlled during the experiments, but it was relatively constant at 25 °C before experiments began and increased to a stable value (approximately 30–34 °C) after the lamps were turned on. RH was maintained manually by adding water vapors generated from a bubbler with zero air as a carrier gas (15 L min<sup>-1</sup>). Other chamber inputs (e.g., H<sub>2</sub>O<sub>2</sub> vapor, NO, seed particles, and  $\alpha$ -pinene) were conducted after the RH reached approximately



95 60%. RH inside the chamber stabilized at approximately 29–43% after the lamps were turned on for about 1 hour due to the increase in temperature.

H<sub>2</sub>O<sub>2</sub> vapor, as the source of OH radical, was introduced into chamber using a bubbler with a flow of zero air (0.09 L min<sup>-1</sup>) passing through H<sub>2</sub>O<sub>2</sub> aqueous solution (30 weight % in water, Sigma-Aldrich) for 1 hour. Ammonium sulfate (AS)/sulfuric acid (SA) solutions with varied NH<sub>4</sub>/SO<sub>4</sub> molar ratios were used to provide various acidities in seed particles.  
100 A complete list of the composition of the seed particles and other initial conditions in all experiments is given in Table 1. The seed particles were generated by atomizing AS/SA aqueous solution using an aerosol generator (model 3706, TSI), dried in a silica gel diffusion dryer, and then size-selected at 150 nm in mobility diameter using a differential mobility analyzer (DMA, model 3081, TSI). Nitric oxide (NO) was added into the chamber from a compressed gas cylinder (9.1 ppm NO in nitrogen) in high-NO<sub>x</sub> experiments, in contrast to low-NO<sub>x</sub> experiments where NO was not added. A micro-syringe was used  
105 to inject approximately 0.25 µL liquid  $\alpha$ -pinene (99+%, Sigma-Aldrich) into the chamber through a stainless steel tube with a zero air at 3 L min<sup>-1</sup>. After achieving the desired experimental conditions for a stable 30 min period, photooxidation reactions were initiated by turning on the lamps. The typical photooxidation time was 6 and 15 hours for high- and low-NO<sub>x</sub> experiments, respectively.

Four experiments were also performed to investigate the effect of aerosol acidity on  $\alpha$ -pinene oxidation products at  
110 different photooxidation stages (Exp. 9–12; Table 1). Photooxidation of  $\alpha$ -pinene was conducted without seed particles in the reaction chamber for 2 and 4 hours under high- and low-NO<sub>x</sub> conditions, respectively. This was followed by turning off the lamps and adding neutral/acidic seed particles into the chamber within 1 hour. The experiments continued for another 6 hours on the reactive uptake of the  $\alpha$ -pinene oxidation products by the newly introduced seed particles in the dark.

The concentration of  $\alpha$ -pinene in the chamber was measured in real-time using a proton-transfer-reaction time-of-flight  
115 mass spectrometer (PTR-ToF-MS, Ionicon Analytik GmbH) (Hansel et al., 1999; Lindinger and Jordan, 1998). The mixing ratios of NO and O<sub>3</sub> were monitored using a NO analyzer (model 42i-Y, Thermo Scientific) and an O<sub>3</sub> monitor (model 202, 2B Technologies), respectively. The particle number size distribution was measured using a scanning mobility particle sizer (SMPS) consisting of a DMA (model 3081, TSI) and a condensation particle counter (model 3776, TSI). The non-refractory chemical composition of the submicron aerosol particles, including organics, sulfate, ammonium, nitrate, and chloride, was  
120 measured using a high resolution time-of-flight aerosol mass spectrometer (HR-ToF-AMS, Aerodyne Research) (DeCarlo et al., 2006). The AMS instrument was operated in a high-sensitivity mode (V-mode) with the data stored at 1 min intervals. The AMS data were processed using the standard ToF-AMS data analysis software (SQUIRREL v1.56D and PIKA v1.15D, <http://cires.colorado.edu/jimenez-group/ToFAMSResources/ToFSoftware/>). The mass concentrations of aerosol species were generated from the PIKA analysis of raw mass spectral data. A collection efficiency value of 0.7 was applied for the AMS  
125 data analysis based upon the comparison of the volume concentrations derived from AMS and SMPS measurements, assuming that particles are spherical and the densities of organics, sulfate, ammonium, and nitrate are 1.4, 1.77, 1.77, and 1.725 g cm<sup>-3</sup>, respectively.



130 SOA yield, which represents the aerosol formation potential of precursor hydrocarbon, was calculated from the ratio of generated SOA mass ( $\Delta M_0$ ) to the reacted  $\alpha$ -pinene mass ( $\Delta HC$ ). The SOA yields and  $\Delta M_0$  presented in Table 1 correspond to the maximum values at the end of each experiment. Organic mass concentrations derived from AMS measurement were 135 wall-loss corrected according to the decay of sulfate particles in the chamber, i.e., by multiplying the ratios of the initial sulfate concentrations to the instantaneously measured sulfate concentrations. This correction assumed that  $\alpha$ -pinene oxidation products condensed on the sulfate particles instead of their self-nucleation. This assumption is appropriate given that organics contributed by self-nucleation was estimated to be less than  $0.1 \mu\text{g cm}^{-3}$  in the studied system. The calculated 140 SOA yield could have been affected by the wall loss of semi-volatile vapors at low  $\alpha$ -pinene loadings, whereas this effect was not taken into account herein. OH concentration in each experiment was estimated from a linear fitting of the first order decay of gaseous  $\alpha$ -pinene by OH radicals, i.e., the difference between the total  $\alpha$ -pinene decay and the  $\alpha$ -pinene consumed by  $O_3$ , as described by Liu et al. (2015). The OH concentrations were calculated to be approximately  $4.3\text{--}5.9 \times 10^6$  and  $0.8\text{--}1.1 \times 10^6$  molecules  $\text{cm}^{-3}$  for experiments under high- and low- $\text{NO}_x$  conditions, respectively.

## 145 3 Results and discussion

### 3.1 $\alpha$ -Pinene SOA formation under high- and low- $\text{NO}_x$ conditions

An increase of  $\alpha$ -pinene SOA mass concentration with the decay of  $\alpha$ -pinene mixing ratio in high- and low- $\text{NO}_x$  150 experiments using  $(\text{NH}_4)_2\text{SO}_4$  seed particles (Exp. 1 and 5 in Table 1) is shown in Figure 1. Under the high- $\text{NO}_x$  condition, the increase of  $\alpha$ -pinene SOA mass was observed shortly after the irradiation started until the end of the experiment (Figure 1a). Gaseous  $\alpha$ -pinene was mostly consumed within approximately 1.5 hours. NO (66 ppbv initially) was consumed in the first 30 min of the irradiation. The formation of  $O_3$  was not suppressed over the experiment.  $O_3$  increased to more than 200 ppb at the end of the experiments, and therefore ozonolysis reactions would have contributed to the formation of  $\alpha$ -pinene SOA. A rough estimation shows that  $\alpha$ -pinene consumed by ozonolysis accounted for in the range of 0–28% of the total  $\alpha$ -pinene decay, as seen from the difference between the total  $\alpha$ -pinene decay and OH consumed  $\alpha$ -pinene in Figure 1a. Nitrate 155 radicals may also have been generated from  $\text{NO}_x$  reactions and have contributed to  $\alpha$ -pinene SOA formation, whereas its direct measurement was not available in this study.

In contrast, under the low- $\text{NO}_x$  condition, the increase of SOA mass concentration and the decay of  $\alpha$ -pinene were relatively slower (Figure 1b). This is most likely due to the low production of OH radicals from  $\text{H}_2\text{O}_2$  photolysis under low- $\text{NO}_x$  condition, that is,  $1.1 \times 10^6$  molecules  $\text{cm}^{-3}$  compared to that of  $5.3 \times 10^6$  molecules  $\text{cm}^{-3}$  under high- $\text{NO}_x$  conditions. A 160 plateau of the generated SOA mass was observed after approximately 12 hours of irradiation, suggesting that SOA formation reached equilibrium after  $\alpha$ -pinene was consumed completely, if the gas-particle partitioning was reversible (Grieshop et al., 2007). NO was less than 0.3 ppbv through the entire experiment. A slight increase of  $O_3$  (up to 30 ppb) was also observed under low- $\text{NO}_x$  conditions, which might have resulted from the photolysis of a small amount of  $\text{NO}_2$  that deposited on the chamber wall. Approximately less than 47% of  $\alpha$ -pinene was consumed by ozonolysis.



160 The  $\alpha$ -pinene SOA yield was 4.0% when using  $(\text{NH}_4)_2\text{SO}_4$  seed particles under high- $\text{NO}_x$  condition, which is a factor of 8.7 lower than that under low- $\text{NO}_x$  condition (34.6%) (Table 1). The relatively lower SOA yield under higher  $\text{NO}_x$  levels is consistent with those reported previously for the photooxidation and ozonolysis of  $\alpha$ -pinene (Eddingsaas et al., 2012; Ng et al., 2007a; Presto et al., 2005). Similar relationships are also observed in the photooxidation of isoprene and aromatic hydrocarbons such as benzene, toluene, and *m*-xylene (Kroll et al., 2006; Ng et al., 2007b). The dependence of  $\alpha$ -pinene SOA yield on  $\text{NO}_x$  level is possibly due to the different gas-phase chemical reactions of the intermediate organic peroxy radicals ( $\text{RO}_2$ ) formed in the initial photooxidation stage.  $\text{RO}_2$  reacted primarily with NO and  $\text{NO}_2$  under high- $\text{NO}_x$  conditions, which would result in the formation of relatively volatile species such as organic nitrates and reduce the overall SOA yield; whereas the reactions of  $\text{RO}_2$  with other peroxy radicals (e.g.,  $\text{RO}_2$  and  $\text{HO}_2$ ) were dominant under low- $\text{NO}_x$  conditions (Kroll et al., 2006; Presto et al., 2005; Xu et al., 2014). Note that the observed difference in SOA yields might 165 also be affected to some extent by other experimental conditions such as the initial  $\alpha$ -pinene concentration, seed loading, and temperature, but  $\text{NO}_x$  level was most likely the primary cause, given that other factors did not vary as much as  $\text{NO}_x$  in these 170 experiments (Table 1).

175 A comparison of SOA yields as a function of the generated SOA mass ( $\Delta M_0$ ) in this study and previous studies of  $\alpha$ -pinene photooxidation is shown in Figure 2. The experimental parameters and SOA yields from previous studies are summarized in Table 2. SOA yields in these studies varied in the range of approximately 1.3–24% in the presence of  $\text{NO}_x$ , in contrast to those of 26–46% without  $\text{NO}_x$ . The SOA yields observed in our study are generally comparable to those reported from previous studies despite with different experimental parameters. The SOA yield under high- $\text{NO}_x$  condition in our study is in particular closest to those with lower  $\alpha$ -pinene level (Ng et al., 2007a; Odum et al., 1996) and at higher temperature (Takekawa et al., 2003). It has been established that low  $\alpha$ -pinene level and high temperature can lead to relatively low SOA 180 yields, which is possibly due to the changes of gas/particle partitioning thermodynamics in the reaction system (Odum et al., 1996; Pankow, 2007; Takekawa et al., 2003). The SOA yield under low- $\text{NO}_x$  conditions here is similar to those reported by Eddingsaas et al. (2012) but lower than those reported by Ng et al. (2007a). The varied SOA yield among these studies most likely depend on different experimental conditions, suggesting that laboratory studies performed under conditions near atmosphere are important for an intercomparison among studies and using those results in air quality models ultimately.

## 185 3.2 Effect of particle acidity on $\alpha$ -pinene SOA yield

### 3.2.1 Dependence of SOA yield on particle acidity

An increase of the  $\alpha$ -pinene SOA yield with an increase of particle acidity was observed under high- $\text{NO}_x$  conditions. The final SOA yields were 5.4%, 6.3%, and 7.3% for acidic particles with the initial  $\text{NH}_4/\text{SO}_4$  molar ratios of 1.0, 0.5, and 0.2, respectively (Table 1). This corresponds to 1.4, 1.6, and 1.8 times the SOA yield for neutral particles (i.e., 4.0%). 190 Conversely, the final SOA yields for acidic particles varied from 27.9% to 35.6% under low- $\text{NO}_x$  conditions, from which a systematic increase in SOA yield with particle acidity was not observed. Clearly,  $\text{NO}_x$  is most likely involved in the acid-catalyzed reactions during  $\alpha$ -pinene photooxidation, such as the formation of organic nitrates from  $\text{RO}_2$  reacting with  $\text{NO}_x$ .



facilitated by particle acidity (as discussed in Sect. 3.4). The dependence of  $\alpha$ -pinene SOA yield on particle acidity under only high- $\text{NO}_x$  conditions in this study is similar to those reported by Eddingsaas et al. (2012), whereas they observed a  
195 smaller increase of SOA yield (approximately 22% compared to 40–80% here) when using acidic particles. The effect of particle acidity on SOA formed from  $\alpha$ -pinene has been reported to be much lower than that for isoprene, e.g., the former one was 8 times lower than the later one (Offenberg et al., 2009).

### 3.2.2 Time scale of acidity effect

200 SOA yield is found to be a strong function of the generated SOA mass ( $\Delta M_0$ ) (Odum et al., 1996). The time-dependent SOA yield as a function of  $\Delta M_0$  for acid and neutral particles under high- and low- $\text{NO}_x$  conditions is shown in Figure 3. Under high- $\text{NO}_x$  conditions, the increase of SOA yield with particle acidity (black through green points) was much stronger in the first hour of photooxidation than in the later period (Figure 3a), suggesting that the acidity effect was more significant in the initial period of photooxidation in this reaction system. This is possibly due to that fresh acidic particles were more  
205 accessible for acid-catalyzed reactions by early  $\alpha$ -pinene oxidation products in the initial stage. A slight decrease in the SOA yield for acidic particles was also observed after the relatively higher SOA yields within the first 30 min. A possible interpretation for such a decrease in yield is that acidic particles were less accessible gradually with increased organic coating of acidic particles. This indicates that the acidity effect is important in particular in the initial stage of acidic particles being introduced. The SOA yields increased nearly linearly with  $\Delta M_0$  after 2 hours of irradiation, suggesting that the growth  
210 of SOA mass continued after the complete consumption of the  $\alpha$ -pinene. This is possibly due to the further oxidation of early-generation products such as carbonyls, hydrocarbonyls, and organic nitrates, and/or the continued partitioning of gas-phase oxidation products into particle-phase. In contrast, the growth curves of SOA yields for acidic particles under low- $\text{NO}_x$  conditions were quite similar to that for neutral particles over the irradiation time (Figure 3b), which again suggests that acidity effect is insignificant under the studied low- $\text{NO}_x$  conditions.

215 The acidity effect on  $\alpha$ -pinene SOA yield was relatively strong in the first hour of irradiation under high- $\text{NO}_x$  conditions, as illustrated above. This effect was characterized more quantitatively as a function of  $\text{NH}_4/\text{SO}_4$  molar ratio, a proxy of particle acidity, in Figure 4. Here, the SOA yields at several specific  $\Delta M_0$  values from 0.7 to 1.9  $\mu\text{g m}^{-3}$  (within the first hour in Figure 3a) are used as it represents the strongest acidity effect observed. As seen in Figure 4, the SOA yield increased nearly linearly with the decrease in the  $\text{NH}_4/\text{SO}_4$  molar ratio. A maximum increase of 220% in SOA yield was  
220 observed for the most acidic particles (i.e.,  $\text{NH}_4/\text{SO}_4$  molar ratio = 0.2) with the  $\Delta M_0$  of 0.5  $\mu\text{g m}^{-3}$  at the irradiation time of approximately 20 min compared to those for neutral particles ( $\text{NH}_4/\text{SO}_4$  molar ratio = 2) (Figure 4). This increase is much higher than the increase in the final SOA yield with particle acidity (i.e., 80% at 6 hours) in the same experiments. Furthermore, the increase in the SOA yield gradually slowed with the increase in organic mass, which is evident by the decreased trend of the slope curve derived from the fitting of SOA yield with  $\text{NH}_4/\text{SO}_4$  molar ratios (Figure 4b). This could  
225 be again explained, at least in part, by acidic particles became less accessible over time with the coating of  $\alpha$ -pinene SOA. Another possible cause is the consumption of sulfate due to the formation of organic sulfates (Surratt et al., 2007a, 2008).



However, we cannot identify organic sulfates clearly based upon the AMS measurement, since their fragmentation results mainly in inorganic sulfate fragments (Farmer et al., 2010).

### 230 3.2.3 Acidity effect on later-generation SOA

Due to organics coating on acidic particles, the effect of particle acidity on SOA formation in the later experimental stage may be underestimated when introducing seed particles before  $\alpha$ -pinene photooxidation, in particular under low- $\text{NO}_x$  conditions with higher SOA yield. The SOA yield growth curves from experiments with seed particles injected after 2 and 4 hours  $\alpha$ -pinene photooxidation under high- and low- $\text{NO}_x$  conditions, respectively, are shown in Figure 5. Here the SOA yield 235 was derived using the same method as that for other experiments (Exp. 1–8 in Table 1), that is, the ratio of  $\Delta M_0/\Delta HC$ . Aerosol particles from the nucleation of gas molecules were not significant in these experiments (less than 50 particles  $\text{cm}^{-3}$ ), and thus the oxidation products were likely present mainly in the gas phase or on the chamber wall prior to adding seed particles.

Organic aerosol mass increased immediately after adding seed particles for all experiments. A slightly higher SOA 240 yield was observed for acidic particles than that for neutral particles in the first 2 hours under both high- and low- $\text{NO}_x$  conditions (Figure 5). This suggests that the formation and/or partitioning of organic aerosols, possibly the mixture of early- and later-generation SOA (although their proportions are unknown based on the available data), were enhanced in the presence of acidic particles even under low- $\text{NO}_x$  conditions, where this effect was not observed previously (as seen in Figure 245 3b). It is postulated that this effect is apparent here since the acidic particles had not been coated previously with early-generation products of  $\alpha$ -pinene photooxidation, which makes the acidic particles accessible to further acid-catalyzed chemistry. Eddingsaas et al. (2012) similarly reported that  $\alpha$ -pinene photooxidation products preferentially partition to highly acidic aerosols when introducing seed particles after OH oxidation under both low- $\text{NO}_x$  and high- $\text{NO}_2$  conditions. Considering there is no discernable acidity effect observed for the low- $\text{NO}_x$  cases previously, it is expected that the actual 250 yield in Figure 5 could be even higher. The results of Figure 5 also indicate that early  $\alpha$ -pinene oxidation products under low- $\text{NO}_x$  condition did not participate in acid catalysis, whereas the later products did. Therefore, acidity effect could be different for  $\alpha$ -pinene SOA products from multiple oxidation steps. Detailed analysis of those products in molecular level is essential to fully understand the acidity effect.

### 3.3 Chemical composition of SOA

The effect of particle acidity on the chemical composition of  $\alpha$ -pinene SOA in high- and low- $\text{NO}_x$  experiments is 255 examined from the distribution of organic fragments in the high-resolution organic aerosol mass spectra. The average fractions of organic fragment groups in the organic aerosol mass spectra for particles of different acidity are shown in Figure 6.  $\text{C}_x\text{H}_y^+$  fragments (accounted for 41–44% of total signal) dominated the organic aerosol mass spectra, followed by  $\text{C}_x\text{H}_y\text{O}_1^+$  (33–35%) and  $\text{C}_x\text{H}_y\text{O}_2^+$  (16–17%) fragments for experiments with varied particle acidity under high- $\text{NO}_x$  conditions (Figure 6a). In contrast,  $\text{C}_x\text{H}_y\text{O}_1^+$  (39–40%) was the most dominant organic fragment, followed by  $\text{C}_x\text{H}_y^+$  (33–36%) and  $\text{C}_x\text{H}_y\text{O}_2^+$



260 (17–19%) fragments under low- $\text{NO}_x$  conditions (Figure 6b). An increase in the fractions of oxygenated fragments ( $\text{C}_x\text{H}_y\text{O}_1^+$  and  $\text{C}_x\text{H}_y\text{O}_2^+$ ) and a decrease in the fraction of hydrocarbon fragments ( $\text{C}_x\text{H}_y^+$ ) were observed under low- $\text{NO}_x$  conditions compared to those under high- $\text{NO}_x$  conditions. Also, lower O/C ratios of  $\alpha$ -pinene SOA were observed under high- $\text{NO}_x$  conditions (0.49–0.54, averaged at the irradiation time of 1–6 hours) compared to those under low- $\text{NO}_x$  conditions (0.60–0.62, averaged at the irradiation time of 2–12 hours). This indicates that less oxygenated  $\alpha$ -pinene SOA was formed in the  
265 presence of high  $\text{NO}_x$  despite the fact that oxidants (i.e., OH and  $\text{O}_3$ ) levels were higher during the high  $\text{NO}_x$  containing experiments (see Table 1 and Figure 1).

The dependence of chemical composition and oxidation state of  $\alpha$ -pinene SOA on  $\text{NO}_x$  level is most likely associated with the gas-phase chemistry of  $\text{RO}_2$ . For instance, peroxy nitrates and organic nitrates formed from the chemical reaction of  $\text{RO}_2$  and  $\text{NO}_x$  are the dominant products under high- $\text{NO}_x$  conditions, whereas organic peroxides and acids formed from  $\text{RO}_2$   
270 with  $\text{HO}_2$  are dominant under low- $\text{NO}_x$  conditions (Xia et al., 2008). SOA formed from photooxidation of isoprene has also been reported to become more oxidized under low- $\text{NO}_x$  conditions, which is contrary to those under high- $\text{NO}_x$  conditions (Xu et al., 2014). Note that the observed variations in organic fragments in Figure 6 generally represent those over the whole photooxidation period in each experiment, since the individual mass spectrum of  $\alpha$ -pinene SOA did not change significantly with irradiation time, as illustrated by the small standard deviations of individual fragment groups.

275 With the increase in particle acidity (i.e.,  $\text{NH}_4/\text{SO}_4$  molar ratio from 2 to 0.2) under high- $\text{NO}_x$  conditions (Figure 6a), the fractions of major fragment ions ( $\text{C}_x\text{H}_y^+$  and  $\text{C}_x\text{H}_y\text{O}_1^+$ ) decreased gradually while  $\text{C}_x\text{H}_y\text{O}_2^+$  fractions increased; a slight increase in the O/C ratio from 0.49 to 0.54 was also observed. This suggests that more oxygenated SOA was possibly formed in the presence of acidic particles under high- $\text{NO}_x$  conditions. A possible interpretation is that particle acidity enhances the formation of more oxygenated SOA in particles such as larger oligomers via acid-catalyzed reactions (Gao et al., 2004),  
280 and/or prompts the partitioning of those oxidation products into particle-phase (Healy et al., 2008), or particle acidity may also help to hydrolyze unsaturated organic molecules. Conversely, there is no systematic change in the chemical composition of  $\alpha$ -pinene SOA with particle acidity under low- $\text{NO}_x$  conditions. Therefore, the effect of particle acidity on the chemical composition of  $\alpha$ -pinene SOA may be important only under the studied high- $\text{NO}_x$  conditions when introducing acidic seed particles before photooxidation, which is consistent with the acidity effect on the yield of  $\alpha$ -pinene SOA (Sect. 3.2). It is  
285 likely that acidic particles coated rapidly by earlier-generation  $\alpha$ -pinene SOA due to the higher SOA yield under low- $\text{NO}_x$  conditions, or the reactions of  $\text{RO}_2$  with  $\text{HO}_2$  and  $\text{RO}_2$  were dominated by termination products that were less affected by particle acidity.

### 3.4 Acid-catalyzed formation of organic nitrates

The formation of organic nitrates from  $\alpha$ -pinene oxidation has been reported previously in the presence of  $\text{NO}_x$  (e.g.,  
290 Atkinson et al., 2000; Albert et al., 2005). Nitrogen (N)-containing organic fragments ( $\text{C}_x\text{H}_y\text{N}_p^+$  and  $\text{C}_x\text{H}_y\text{O}_z\text{N}_p^+$ ) accounted for less than 10% of total organic signal in our studied conditions. These fragments were most likely contributed by organic nitrates generated from the reactions of early  $\alpha$ -pinene oxidation intermediate ( $\text{RO}_2$ ) with  $\text{NO}$  and  $\text{NO}_2$ . Organic nitrates



likely account for an even higher fraction of the total organic aerosols, since their fragmentation would primarily contribute to inorganic nitrate fragments ( $\text{NO}^+/\text{NO}_2^+$ ) (Farmer et al., 2010). Organic nitrates yields have been reported to range from 295 approximately 1% up to more than 20% for  $\alpha$ -pinene oxidation (Aschmann et al., 2002; Nozière et al., 1999; Rindelaub et al., 2015). The organic nitrates yield in our study was roughly estimated to be in the range of 0.5–1.4%, which was calculated from the ratio of the summed inorganic and organic N-containing fragments ( $\text{NO}^+ + \text{NO}_2^+ + \text{C}_x\text{H}_y\text{N}_p^+ + \text{C}_x\text{H}_y\text{O}_z\text{N}_p^+$ ) mass to  $\Delta\text{HC}$ .

Interestingly, both the fractions of  $\text{C}_x\text{H}_y\text{N}_p^+$  and  $\text{C}_x\text{H}_y\text{O}_z\text{N}_p^+$  fragments increased gradually with the increase in particle 300 acidity under high- $\text{NO}_x$  conditions (Figure 6a), which is distinct from those without an apparent change under low- $\text{NO}_x$  conditions (Figure 6b). The growth curves of the total N-containing organic fragments (sum of  $\text{C}_x\text{H}_y\text{N}_x^+$  and  $\text{C}_x\text{H}_y\text{O}_z\text{N}_p^+$ ) for different acidic particles under high- $\text{NO}_x$  conditions are shown in Figure 7a. The absolute mass concentrations of total N-containing organic fragments were also enhanced with particle acidity over the irradiation period. These results indicate that 305 organic nitrates were formed heterogeneously through a mechanism catalyzed by aerosol acidity or that acidic conditions facilitate the partitioning of gas phase nitrates into particle phase under high- $\text{NO}_x$  conditions. It has been reported that particle acidity may enhance the partitioning of gaseous organic nitrates into the particle phase due to the acid-catalyzed hydrolysis of particle-phase organic nitrates, especially under high RH and aqueous conditions (Day et al., 2010; Hu et al., 2011; Liu et al., 2012; Rindelaub et al., 2015). However, the hydrolysis of organic nitrates in the particle phase results in 310 their conversion to alcohols and nitric acid, which would lead to decrease in both their gas and particle phase amounts (Rindelaub et al., 2015). This is inconsistent with the observed increase in organic nitrate fragments with increasing acidity. Therefore, acid-catalyzed formation of organic nitrates also very likely contributed to the observed enhancement of N-containing organic fragments with particle acidity.

The time-dependent mass concentrations of  $\text{NO}^+$  and  $\text{NO}_2^+$  fragments for varied acidic particles under high- $\text{NO}$  315 conditions are also shown in Figure 7b. The mass concentrations of the  $\text{NO}^+$  fragment for acidic particles were higher than those of neutral particles, whereas no apparent difference in the  $\text{NO}_2^+$  fragment was observed for particles with varied acidity. Therefore, the enhanced organic nitrates by particle acidity might contribute mainly to the increase in  $\text{NO}^+$  fragment. Large 320 relative contribution of organic nitrates to the nominal inorganic nitrate fragments is demonstrated by a higher  $\text{NO}^+/\text{NO}_2^+$  ratio than those of pure ammonium nitrate (Bae et al., 2007; Farmer et al., 2010; Fry et al., 2009). The average  $\text{NO}^+/\text{NO}_2^+$  ratio was 9.13, 9.28, 9.31, and 10.44 for particles with initial  $\text{NH}_4/\text{SO}_4$  molar ratio of 2, 1, 0.5, and 0.2, respectively. These values are significantly higher than  $2.6 \pm 0.2$  from the current AMS measurement of pure ammonium nitrate, but very similar to that of  $11 \pm 8$  reported for  $\text{NO}_3$  oxidation of  $\alpha$ -pinene, from which organic nitrates were likely the dominant aerosol component (Bruns et al., 2010). An increasing  $\text{NO}^+/\text{NO}_2^+$  ratio again suggests that organic nitrates were enhanced with the increase in particle acidity under high- $\text{NO}_x$  conditions.



#### 4 Implications

325 This study investigated the effect of particle acidity on the yield and chemical composition of  $\alpha$ -pinene SOA from OH-initiated photooxidation in a photochemical reaction chamber. A nearly linear increase of  $\alpha$ -pinene SOA yield with the increase in particle acidity was observed under high- $\text{NO}_x$  conditions, which is contrary to the insignificant acidity effect under low- $\text{NO}_x$  conditions. The acidity effect was relatively strong in the early photooxidation stages under high- $\text{NO}_x$  conditions, and this effect decreased gradually with the growth of SOA mass. This may be explained by a reduced  
330 accessibility of the SOA partitioning species to the acidic particles for acid-catalyzed chemistry, possibly as a result of the SOA coating. Given that the  $\alpha$ -pinene loading used in this study was low, similar phenomenon may also occur in the atmosphere. Consequently, an ambient acidity effect is likely stronger for newly formed particles and/or freshly formed sulfate coating. Therefore, the time scale of SOA formation with respect to acidity effects is expected to be an important factor for field studies measuring acidity effect in the atmosphere.

335 More oxygenated SOA was formed with the increase of particle acidity under high- $\text{NO}_x$  conditions. Since aerosol acidity could affect the oxidation state of aerosol particles and alter their chemical composition and other properties as demonstrated here, this may be an important process in the atmosphere and deserve further investigation. The formation of SOA from later-generation gas phase products was enhanced by particle acidity even under low- $\text{NO}_x$  conditions when introducing acidic seed particles after  $\alpha$ -pinene photooxidation. This suggests that the overall acidity effect on the formation  
340 of SOA could be underestimated, and that more systematic studies are necessary to evaluate the acidity effect on SOA generated from multiple oxidation steps. Organic nitrates in these experiments may be formed heterogeneously through a mechanism catalyzed by particle acidity and/or the acidic conditions facilitate the partitioning of gas phase nitrates into the particle phase under high- $\text{NO}_x$  conditions. This implies that aerosol acidity could also be of importance in the atmosphere by altering the deposition patterns/rates of gas phase  $\text{NO}_x$  via its conversion to particle nitrates with differing atmospheric  
345 lifetimes.

Finally, further studies on SOA formation from various other hydrocarbons under conditions near ambient atmospheric levels will be valuable in evaluating the acidity effect more accurately, and to ultimately incorporate such effects into regional air quality model for improved SOA prediction.

#### Acknowledgments

350 This study was funded by the Joint Oil Sands Monitoring Program between Alberta Environment and Sustainable Resource Development and Environment Canada.



## References

Aschmann, S. M., Atkinson, R. and Arey, J.: Products of reaction of OH radicals with alpha-pinene, *J. Geophys. Res.*, 107(D14), 4191, doi:10.1029/2001JD001098, 2002.

355 Atkinson, R.: Atmospheric chemistry of VOCs and NO<sub>x</sub>, *Atmos. Environ.*, doi:10.1016/S1352-2310(99)00460-4, 2000.

Bae, M. S., Schwab, J. J., Zhang, Q., Hogrefe, O., Dermerjian, K. L., Weimer, S., Rhoads, K., Orsini, D., Venkatachari, P. and Hopke, P. K.: Interference of organic signals in highly time resolved nitrate measurements by low mass resolution aerosol mass spectrometry, *J. Geophys. Res. Atmos.*, 112, 1–16, doi:10.1029/2007JD008614, 2007.

360 Barsanti, K. C. and Pankow, J. F.: Thermodynamics of the formation of atmospheric organic particulate matter by accretion reactions—Part 1: aldehydes and ketones, *Atmos. Environ.*, 38(26), 4371–4382, doi:10.1016/j.atmosenv.2004.03.035, 2004.

Bruns, E. a., Perraud, V., Zelenyuk, A., Ezell, M. J., Johnson, S. N., Yu, Y., Imre, D., Finlayson-Pitts, B. J. and Alexander, M. L.: Comparison of FTIR and particle mass spectrometry for the measurement of particulate organic nitrates, *Environ. Sci. Technol.*, 44(3), 1056–1061, doi:10.1021/es9029864, 2010.

365 Casale, M. T., Richman, A. R., Elrod, M. J., Garland, R. M., Beaver, M. R. and Tolbert, M. a.: Kinetics of acid-catalyzed aldol condensation reactions of aliphatic aldehydes, *Atmos. Environ.*, 41, 6212–6224, doi:10.1016/j.atmosenv.2007.04.002, 2007.

Chu, B., Liu, Y., Li, J., Takekawa, H., Liggio, J., Li, S. M., Jiang, J., Hao, J. and He, H.: Decreasing effect and mechanism of FeSO<sub>4</sub> seed particles on secondary organic aerosol in  $\alpha$ -pinene photooxidation, *Environ. Pollut.*, 193, 88–93, doi:10.1016/j.envpol.2014.06.018, 2014.

370 Day, D. a., Liu, S., Russell, L. M. and Ziemann, P. J.: Organonitrate group concentrations in submicron particles with high nitrate and organic fractions in coastal southern California, *Atmos. Environ.*, 44(16), 1970–1979, doi:10.1016/j.atmosenv.2010.02.045, 2010.

Decarlo, P. F., Kimmel, J. R., Trimborn, A., Northway, M. J., Jayne, J. T., Aiken, A. C., Gonin, M., Fuhrer, K., Horvath, T., Docherty, K. S., Worsnop, D. R. and Jimenez, J. L.: Aerosol Mass Spectrometer, 78(24), 8281–8289, doi:8410.1029/2001JD001213.Analytical, 2006.

375 Eddingsaas, N. C., Loza, C. L., Yee, L. D., Chan, M., Schilling, K. a., Chhabra, P. S., Seinfeld, J. H. and Wennberg, P. O.:  $\alpha$ -pinene photooxidation under controlled chemical conditions-Part 2: SOA yield and composition in low-and high-NO x environments, *Atmos. Chem. Phys.*, 12(16), 7413–7427, doi:10.5194/acp-12-7413-2012, 2012.

Farmer, D. K., Matsunaga, a, Docherty, K. S., Surratt, J. D., Seinfeld, J. H., Ziemann, P. J. and Jimenez, J. L.: Response of an aerosol mass spectrometer to organonitrates and organosulfates and implications for atmospheric chemistry., *Proc. Natl. Acad. Sci. U.S.A.*, 107, 6670–6675, doi:10.1073/pnas.0912340107, 2010.

Fry, J. L., Rollins, a W., Wooldridge, P. J., Brown, S. S., Fuchs, H. and Dub, W.: Organic nitrate and secondary organic aerosol yield from NO<sub>3</sub> oxidation of  $\beta$ -pinene evaluated using a gas-phase kinetics/aerosol partitioning model, *Atmos. Chem. Phys.*, 9(4), 1431–1449, doi:10.5194/acp-9-1431-2009, 2009.



385 Gao, S., Ng, N. L., Keywood, M., Varutbangkul, V., Bahreini, R., Nenes, A., He, J., Yoo, K. Y., Beauchamp, J. L., Hodyss, R. P., Flagan, R. C. and Seinfeld, J. H.: Particle phase acidity and oligomer formation in secondary organic aerosol, *Environ. Sci. Technol.*, 38(24), 6582–6589, doi:10.1021/es049125k, 2004.

Garland, R. M., Elrod, M. J., Kincaid, K., Beaver, M. R., Jimenez, J. L. and Tolbert, M. a.: Acid-catalyzed reactions of hexanal on sulfuric acid particles: Identification of reaction products, *Atmos. Environ.*, 40, 6863–6878, 390 doi:10.1016/j.atmosenv.2006.07.009, 2006.

Grieshop, A. P., Donahue, N. M. and Robinson, A. L.: Is the gas-particle partitioning in alpha-pinene secondary organic aerosol reversible?, *Geophys. Res. Lett.*, 34(14), L14810, doi:10.1029/2007GL029987, 2007.

Guenther, a. B., Jiang, X., Heald, C. L., Sakulyanontvittaya, T., Duhl, T., Emmons, L. K. and Wang, X.: The model of emissions of gases and aerosols from nature version 2.1 (MEGAN2.1): An extended and updated framework for modeling 395 biogenic emissions, *Geosci. Model Dev.*, 5, 1471–1492, doi:10.5194/gmd-5-1471-2012, 2012.

Hallquist, M., Wenger, J. C., Baltensperger, U., Rudich, Y., Simpson, D., Claeys, M., Dommen, J., Donahue, N. M., George, C., Goldstein, A. H., Hamilton, J. F., Herrmann, H., Hoffmann, T., Iinuma, Y., Jang, M., Jenkin, M. E., Jimenez, J. L., Kiendler-Scharr, A., Maenhaut, W., McFiggans, G., Mentel, T. F., Monod, A., Prévôt, A. S. H., Seinfeld, J. H., Surratt, J. D., Szmigielski, R. and Wildt, J.: The formation, properties and impact of secondary organic aerosol: current and emerging 400 issues, *Atmos. Chem. Phys.*, 9(14), 5155–5236, doi:10.5194/acp-9-5155-2009, 2009.

Hansel, A., Jordan, A., Warneke, C., Holzinger, R., Wisthaler, A. and Lindner, W.: Proton-transfer-reaction mass spectrometry (PTR-MS): on-line monitoring of volatile organic compounds at volume mixing ratios of a few pptv, *Plasma Sources Sci. Technol.*, 8(2), 332–336, doi:10.1088/0963-0252/8/2/314, 1999.

Hawkins, L. N., Russell, L. M., Covert, D. S., Quinn, P. K. and Bates, T. S.: Carboxylic acids, sulfates, and organosulfates in 405 processed continental organic aerosol over the southeast Pacific Ocean during VOCALS-REx 2008, *J. Geophys. Res. Atmos.*, 115, 1–16, doi:10.1029/2009JD013276, 2010.

Healy, R. M., Wenger, J. C., Metzger, a., Duplissy, J., Kalberer, M. and Dommen, J.: Gas/particle partitioning of carbonyls in the photooxidation of isoprene and 1,3,5-trimethylbenzene, *Atmos. Chem. Phys.*, 8(12), 3215–3230, doi:10.5194/acp-8-3215-2008, 2008.

410 Hu, K. S., Darer, a. I. and Elrod, M. J.: Thermodynamics and kinetics of the hydrolysis of atmospherically relevant organonitrates and organosulfates, *Atmos. Chem. Phys.*, 11, 8307–8320, doi:10.5194/acp-11-8307-2011, 2011.

Iinuma, Y., Böge, O., Gnauk, T. and Herrmann, H.: Aerosol-chamber study of the  $\alpha$ -pinene/O<sub>3</sub> reaction: influence of particle acidity on aerosol yields and products, *Atmos. Environ.*, 38(5), 761–773, doi:10.1016/j.atmosenv.2003.10.015, 2004.

Jang, M., Czoschke, N. M., Lee, S. and Kamens, R. M.: Heterogeneous atmospheric aerosol production by acid-catalyzed 415 particle-phase reactions., *Science*, 298(2002), 814–817, doi:10.1126/science.1075798, 2002.

Jang, M., Czoschke, N. M. and Northcross, A. L.: Atmospheric organic aerosol production by heterogeneous acid-catalyzed reactions, *ChemPhysChem*, 5, 1646–1661, doi:10.1002/cphc.200301077, 2004.



Jonsson, Å. M., Hallquist, M. and Ljungström, E.: Impact of humidity on the ozone initiated oxidation of limonene,  $\Delta$ 3-carene, and  $\alpha$ -pinene, *Environ. Sci. Technol.*, 40(1), 188–194, doi:10.1021/es051163w, 2006.

420 Kanakidou, M., Seinfeld, J. H., Pandis, S. N., Barnes, I., Dentener, F. J., Facchini, M. C., Van Dingenen, R., Ervens, B., Nenes, a., Nielsen, C. J., Swietlicki, E., Putaud, J. P., Balkanski, Y., Fuzzi, S., Horth, J., Moortgat, G. K., Winterhalter, R., Myhre, C. E. L., Tsigaridis, K., Vignati, E., Stephanou, E. G. and Wilson, J.: Organic aerosol and global climate modelling: a review, *Atmos. Chem. Phys.*, 5, 1053–1123, doi:10.5194/acp-5-1053-2005, 2005.

425 Kim, H. and Paulson, S. E.: Real refractive indices and volatility of secondary organic aerosol generated from photooxidation and ozonolysis of limonene,  $\alpha$ -pinene and toluene, *Atmos. Chem. Phys.*, 13, 7711–7723, doi:10.5194/acp-13-7711-2013, 2013.

Kleindienst, T. E., Edney, E. O., Lewandowski, M., Offenberg, J. H. and Jaoui, M.: Secondary organic carbon and aerosol yields from the irradiations of isoprene and  $\alpha$ -pinene in the presence of NO<sub>x</sub> and SO<sub>2</sub>, *Environ. Sci. Technol.*, 40(12), 3807–3812, doi:10.1021/es052446r, 2006.

430 Kristensen, K., Cui, T., Zhang, H., Gold, a., Glasius, M. and Surratt, J. D.: Dimers in  $\alpha$ -pinene secondary organic aerosol: Effect of hydroxyl radical, ozone, relative humidity and aerosol acidity, *Atmos. Chem. Phys.*, 14, 4201–4218, doi:10.5194/acp-14-4201-2014, 2014.

Kroll, J. H., Ng, N. L., Murphy, S. M., Flagan, R. C. and Seinfeld, J. H.: Secondary organic aerosol formation from isoprene photooxidation, *Environ. Sci. Technol.*, 40(3), 1869–1877, doi:10.1021/es0524301, 2006.

435 Kroll, J. H., Ng, N. L., Murphy, S. M., Varutbangkul, V., Flagan, R. C. and Seinfeld, J. H.: Chamber studies of secondary organic aerosol growth by reactive uptake of simple carbonyl compounds, *J. Geophys. Res. Atmos.*, 110, 1–10, doi:10.1029/2005JD006004, 2005.

Lewandowski, M., Jaoui, M., Offenberg, J. H., Krug, J. D. and Kleindienst, T. E.: Atmospheric oxidation of isoprene and 1,3-butadiene: Influence of aerosol acidity and relative humidity on secondary organic aerosol, *Atmos. Chem. Phys.*, 15, 440 3773–3783, doi:10.5194/acp-15-3773-2015, 2015.

Li, Y. J., Lee, A. K. Y., Lau, A. P. S. and Chan, C. K.: Accretion reactions of octanal catalyzed by sulfuric acid: Product identification, reaction pathways, and atmospheric implications, *Environ. Sci. Technol.*, 42(19), 7138–7145, doi:10.1021/es7031373, 2008.

Liggio, J., Li, S. M. and McLaren, R.: Heterogeneous reactions of glyoxal on particulate matter: Identification of acetals and 445 sulfate esters, *Environ. Sci. Technol.*, 39(6), 1532–1541, doi:10.1021/es048375y, 2005.

Liggio, J. and Li, S. M.: Reactive uptake of pinonaldehyde on acidic aerosols, *J. Geophys. Res. Atmos.*, 111, 1–12, doi:10.1029/2005JD006978, 2006.

Lin, P., Yu, J. Z., Engling, G. and Kalberer, M.: Organosulfates in humic-like substance fraction isolated from aerosols at seven locations in East Asia: A study by ultra-high-resolution mass spectrometry, *Environ. Sci. Technol.*, 46, 13118–13127, 450 doi:10.1021/es303570v, 2012.



Lindinger, W. and Jordan, A.: Proton-transfer-reaction mass spectrometry (PTR-MS): on-line monitoring of volatile organic compounds at pptv levels, *Chem. Soc. Rev.*, 27(5), 347, doi:10.1039/a827347z, 1998.

Liu, S., Shilling, J. E., Song, C., Hiranuma, N., Zaveri, R. a. and Russell, L. M.: Hydrolysis of Organonitrate Functional Groups in Aerosol Particles, *Aerosol Sci. Technol.*, 46, 1359–1369, doi:10.1080/02786826.2012.716175, 2012.

455 Liu, Y., Liggio, J., Staebler, R. and Li, S.-M.: Reactive uptake of ammonia to secondary organic aerosols: kinetics of organonitrogen formation, *Atmos. Chem. Phys.*, 15(23), 13569–13584, doi:10.5194/acp-15-13569-2015, 2015.

Ng, N. L., Canagaratna, M. R., Zhang, Q., Jimenez, J. L., Tian, J., Ulbrich, I. M., Kroll, J. H., Docherty, K. S., Chhabra, P. S., Bahreini, R., Murphy, S. M., Seinfeld, J. H., Hildebrandt, L., Donahue, N. M., Decarlo, P. F., Lanz, V. a., Prévôt, A. S. H., Dinar, E., Rudich, Y. and Worsnop, D. R.: Organic aerosol components observed in Northern Hemispheric datasets from 460 Aerosol Mass Spectrometry, *Atmos. Chem. Phys.*, 10(10), 4625–4641, doi:10.5194/acp-10-4625-2010, 2010.

Ng, N. L., Chhabra, P. S., Chan, a. W. H., Surratt, J. D., Kroll, J. H., Kwan, a. J., McCabe, D. C., Wennberg, P. O., Sorooshian, A., Murphy, S. M., Dalleska, N. F., Flagan, R. C. and Seinfeld, J. H.: Effect of NO<sub>x</sub> level on secondary organic aerosol (SOA) formation from the photooxidation of terpenes, *Atmos. Chem. Phys.*, 7(19), 5159–5174, doi:10.5194/acpd-7-10131-2007, 2007a.

465 Ng, N. L., Kroll, J. H., Chan, a W. H., Chhabra, P. S., Flagan, R. C. and Seinfeld, J. H.: Secondary organic aerosol formation from m-xylene, toluene, and benzene, *Atmos. Chem. Phys.*, 7(3), 3909–3922, doi:10.5194/acp-7-3909-2007, 2007b.

Northcross, A. L. and Jang, M.: Heterogeneous SOA yield from ozonolysis of monoterpenes in the presence of inorganic acid, *Atmos. Environ.*, 41(7), 1483–1493, doi:10.1016/j.atmosenv.2006.10.009, 2007.

Nozière, B., Barnes, I. and Becker, K.-H.: Product study and mechanisms of the reactions of  $\alpha$ -pinene and of pinonaldehyde 470 with OH radicals, *J. Geophys. Res.*, 104, 23645, doi:10.1029/1999JD900778, 1999.

Odum, J. R., Hoffmann, T., Bowman, F., Collins, D., Flagan, R. C. and Seinfeld, J. H.: Gas/Particle Partitioning and Secondary Organic Aerosol Yields, *Environ. Sci. Technol.*, 30(8), 2580–2585, doi:10.1021/es950943+, 1996.

Offenberg, J. H., Wandowski, M., Edney, E. O., Kleindienst, T. E. and Jaoui, M.: Influence of aerosol acidity on the 475 formation of secondary organic aerosol from biogenic precursor hydrocarbons, *Environ. Sci. Technol.*, 43(20), 7742–7747, doi:10.1021/es901538e, 2009.

Pankow, J. F.: An absorption model of the gas/aerosol partitioning involved in the formation of secondary organic aerosol, *Atmos. Environ.*, 41, 75–79, doi:10.1016/j.atmosenv.2007.10.060, 2007.

Peltier, R. E., Sullivan, a. P., Weber, R. J., Wollny, a. G., Holloway, J. S., Brock, C. a., de Gouw, J. a. and Atlas, E. L.: No 480 evidence for acid-catalyzed secondary organic aerosol formation in power plant plumes over metropolitan Atlanta, Georgia, *Geophys. Res. Lett.*, 34, 1–5, doi:10.1029/2006GL028780, 2007.

Pfaffenberger, L., Barmet, P., Slowik, J. G., Praplan, A. P., Dommen, J., Prévôt, A. S. H. and Baltensperger, U.: The link between organic aerosol mass loading and degree of oxygenation: An  $\alpha$ -pinene photooxidation study, *Atmos. Chem. Phys.*, doi:10.5194/acp-13-6493-2013, 2013.



Presto, A. A., Huff Hartz, K. E. and Donahue, N. M.: Secondary Organic Aerosol Production from Terpene Ozonolysis. 2.  
485 Effect of NO<sub>x</sub> Concentration, Environ. Sci. Technol., 39(18), 7046–7054, doi:10.1021/es050400s, 2005.

Rengarajan, R., Sudheer, a. K. and Sarin, M. M.: Aerosol acidity and secondary organic aerosol formation during wintertime over urban environment in western India, Atmos. Environ., 45(11), 1940–1945, doi:10.1016/j.atmosenv.2011.01.026, 2011.

Rindelaub, J. D., McAvey, K. M. and Shepson, P. B.: The photochemical production of organic nitrates from  $\alpha$ -pinene and loss via acid-dependent particle phase hydrolysis, Atmos. Environ., 100, 193–201, doi:10.1016/j.atmosenv.2014.11.010,  
490 2015.

Saathoff, H., Naumann, K.-H., Moehler, O., Jonsson, a M., Hallquist, M., Kiendler-Scharr, a, Mentel, T. F., Tillmann, R. and Schurath, U.: Temperature dependence of yields of secondary organic aerosols from the ozonolysis of alpha-pinene and limonene, Atmos. Chem. Phys., 9(5), 1551–1577, doi:10.5194/acp-9-1551-2009, 2009.

Shilling, J. E., Chen, Q., King, S. M., Rosenoern, T., Kroll, J. H., Worsnop, D. R., DeCarlo, P. F., Aiken, a. C., Sueper, D.,  
495 Jimenez, J. L. and Martin, S. T.: Loading-dependent elemental composition of  $\alpha$ -pinene SOA particles, Atmos. Chem. Phys., 9, 771–782, doi:10.5194/acp-9-771-2009, 2009.

Song, C., Gyawali, M., Zaveri, R. a., Shilling, J. E. and Arnott, W. P.: Light absorption by secondary organic aerosol from  $\alpha$ -pinene: Effects of oxidants, seed aerosol acidity, and relative humidity, J. Geophys. Res. Atmos., 118, 11741–11749, doi:10.1002/jgrd.50767, 2013.

500 Surratt, J. D., Gómez-González, Y., Chan, A. W. H., Vermeylen, R., Shahgholi, M., Kleindienst, T. E., Edney, E. O., Offenberg, J. H., Lewandowski, M., Jaoui, M., Maenhaut, W., Claeys, M., Flagan, R. C. and Seinfeld, J. H.: Organosulfate Formation in Biogenic Secondary Organic Aerosol, J. Phys. Chem. A, 112(36), 8345–8378, doi:10.1021/jp802310p, 2008.

Surratt, J. D., Kroll, J. H., Kleindienst, T. E., Edney, E. O., Claeys, M., Sorooshian, A., Ng, N. L., Offenberg, J. H., Lewandowski, M., Jaoui, M., Flagan, R. C. and Seinfeld, J. H.: Evidence for organosulfates in secondary organic aerosol,  
505 Environ. Sci. Technol., 41(2), 517–527, doi:10.1021/es062081q, 2007a.

Surratt, J. D., Lewandowski, M., Offenberg, J. H., Jaoui, M., Kleindienst, T. E., Edney, E. O. and Seinfeld, J. H.: Effect of acidity on secondary organic aerosol formation from isoprene, Environ. Sci. Technol., 41(15), 5363–5369, doi:10.1021/es0704176, 2007b.

Takahama, S., Davidson, C. I. and Pandis, S. N.: Semicontinuous measurements of organic carbon and acidity during the  
510 Pittsburgh Air Quality Study: Implications for acid-catalyzed organic aerosol formation, Environ. Sci. Technol., 40(7), 2191–2199, doi:10.1021/es050856+, 2006.

Takekawa, H., Minoura, H. and Yamazaki, S.: Temperature dependence of secondary organic aerosol formation by photo-oxidation of hydrocarbons, Atmos. Environ., 37, 3413–3424, doi:10.1016/S1352-2310(03)00359-5, 2003.

Tanner, R. L., Olszyna, K. J., Edgerton, E. S., Knipping, E. and Shaw, S. L.: Searching for evidence of acid-catalyzed  
515 enhancement of secondary organic aerosol formation using ambient aerosol data, Atmos. Environ., 43, 3440–3444, doi:10.1016/j.atmosenv.2009.03.045, 2009.



Xia, A. G., Michelangeli, D. V. and Makar, P. a.: Box model studies of the secondary organic aerosol formation under different HC/NO x conditions using the subset of the Master Chemical Mechanism for  $\alpha$ -pinene oxidation, *J. Geophys. Res.*, 113, D10301, doi:10.1029/2007JD008726, 2008.

520 Xu, L., Kollman, M. S., Song, C., Shilling, J. E. and Ng, N. L.: Effects of NO<sub>x</sub> on the volatility of secondary organic aerosol from isoprene photooxidation, *Environ. Sci. Technol.*, 48(4), 2253–2262, doi:10.1021/es404842g, 2014.

Yasmeen, F., Vermeylen, R., Maurin, N., Perraudin, E., Doussin, J. F. and Claeys, M.: Characterisation of tracers for aging of  $\alpha$ -pinene secondary organic aerosol using liquid chromatography/negative ion electrospray ionisation mass spectrometry, *Environ. Chem.*, 9(3), 236–246, doi:10.1071/EN11148, 2012.

525 Zhang, H., Worton, D. R., Lewandowski, M., Ortega, J., Rubitschun, C. L., Park, J. H., Kristensen, K., Campuzano-Jost, P., Day, D. a., Jimenez, J. L., Jaoui, M., Offenberg, J. H., Kleindienst, T. E., Gilman, J., Kuster, W. C., De Gouw, J., Park, C., Schade, G. W., Frossard, A. a., Russell, L., Kaser, L., Jud, W., Hansel, A., Cappellin, L., Karl, T., Glasius, M., Guenther, A., Goldstein, A. H., Seinfeld, J. H., Gold, A., Kamens, R. M. and Surratt, J. D.: Organosulfates as tracers for secondary organic aerosol (SOA) formation from 2-methyl-3-buten-2-ol (MBO) in the atmosphere, *Environ. Sci. Technol.*, 46, 9437–9446, 530 doi:10.1021/es301648z, 2012.

Zhang, Q., Jimenez, J. L., Canagaratna, M. R., Allan, J. D., Coe, H., Ulbrich, I., Alfarra, M. R., Takami, a., Middlebrook, a. M., Sun, Y. L., Dzepina, K., Dunlea, E., Docherty, K., DeCarlo, P. F., Salcedo, D., Onasch, T., Jayne, J. T., Miyoshi, T., Shimono, a., Hatakeyama, S., Takegawa, N., Kondo, Y., Schneider, J., Drewnick, F., Borrmann, S., Weimer, S., Demerjian, K., Williams, P., Bower, K., Bahreini, R., Cottrell, L., Griffin, R. J., Rautiainen, J., Sun, J. Y., Zhang, Y. M. and Worsnop, 535 D. R.: Ubiquity and dominance of oxygenated species in organic aerosols in anthropogenically-influenced Northern Hemisphere midlatitudes, *Geophys. Res. Lett.*, 34, doi:10.1029/2007GL029979, 2007a.

Zhang, Q., Jimenez, J. L., Worsnop, D. R. and Canagaratna, M.: A case study of urban particle acidity and its influence on secondary organic aerosol, *Environ. Sci. Technol.*, 41, 3213–3219, doi:doi:10.1021/Es061812j, 2007b.

540 Zhou, S., Wang, Z., Gao, R., Xue, L., Yuan, C., Wang, T. and Gao, X.: Formation of secondary organic carbon and long-range transport of carbonaceous aerosols at Mount Heng in South China, *Atmos. Environ.*, 63, 203–212, doi:10.1016/j.atmosenv.2012.09.021, 2012.



## Tables

**Table 1. Experimental conditions and SOA yields from OH-initiated photooxidation of  $\alpha$ -pinene under high- and low-NO<sub>x</sub> conditions.**

545

Exp.	Initial seed composition <sup>a</sup> mole kg <sup>-1</sup>	Molar ratio <sup>b</sup> (NH <sub>4</sub> /SO <sub>4</sub> )	Temp. (°C)	RH (%)	Seed conc. (μg cm <sup>-3</sup> )	NO (ppbv)	$\alpha$ -pinene (ppbv)	ΔHC (μg m <sup>-3</sup> )	ΔM <sub>0</sub> (μg m <sup>-3</sup> )	Yield (%)
<b>High-NO<sub>x</sub></b>										
1	(NH <sub>4</sub> ) <sub>2</sub> SO <sub>4</sub> (no liquid phase)	2	24–31 <sup>c</sup>	47–29 <sup>c</sup>	4.4	66	15.9	84.2	3.4	4.0±0.1
2	H <sup>+</sup> =5.3, NH <sub>4</sub> <sup>+</sup> =27.8, HSO <sub>4</sub> <sup>-</sup> =22.7, SO <sub>4</sub> <sup>2-</sup> =5.2	1	23–30	58–34	8.4	69	17.6	93.4	5.0	5.4±0.1
3	H <sup>+</sup> =9.1, NH <sub>4</sub> <sup>+</sup> =6.9, HSO <sub>4</sub> <sup>-</sup> =11.8, SO <sub>4</sub> <sup>2-</sup> =2.1	0.5	24–30	61–38	6.3	68	13.6	71.8	4.6	6.3±0.2
4	H <sup>+</sup> =10.6, NH <sub>4</sub> <sup>+</sup> =1.8, HSO <sub>4</sub> <sup>-</sup> =8.7, SO <sub>4</sub> <sup>2-</sup> =1.9	0.2	26–34	58–33	7.9	72	17.0	89.9	6.6	7.3±0.2
<b>Low-NO<sub>x</sub></b>										
5	(NH <sub>4</sub> ) <sub>2</sub> SO <sub>4</sub> (no liquid phase)	2	25–32	67–43	12.6	<0.3	19.6	96.7	33.5	34.6±1.1
6	H <sup>+</sup> =5.2, NH <sub>4</sub> <sup>+</sup> =28.6, HSO <sub>4</sub> <sup>-</sup> =23.1, SO <sub>4</sub> <sup>2-</sup> =5.4	1	25–32	64–37	12.6	<0.3	17.4	79.1	22.1	27.9±1.2
7	H <sup>+</sup> =9.1, NH <sub>4</sub> <sup>+</sup> =7.0, HSO <sub>4</sub> <sup>-</sup> =11.8, SO <sub>4</sub> <sup>2-</sup> =2.1	0.5	26–33	64–38	11.9	<0.3	19.3	92.6	33.0	35.6±1.2
8	H <sup>+</sup> =10.5, NH <sub>4</sub> <sup>+</sup> =2.1, HSO <sub>4</sub> <sup>-</sup> =8.9, SO <sub>4</sub> <sup>2-</sup> =1.9	0.2	24–33	66–36	11.4	<0.3	19.5	88.6	27.6	31.2±1.9
<b>Adding seeds after photooxidation</b>										
9	(NH <sub>4</sub> ) <sub>2</sub> SO <sub>4</sub> (no liquid phase)	2	23–31	57–34	9.7	82	20.4	109.3	1.4	1.5±0.1
10	H <sup>+</sup> =9.1, NH <sub>4</sub> <sup>+</sup> =6.9, HSO <sub>4</sub> <sup>-</sup> =11.8, SO <sub>4</sub> <sup>2-</sup> =2.1	0.5	24–31	56–33	12.2	72	18.5	98.9	1.1	1.3±0.1
11	(NH <sub>4</sub> ) <sub>2</sub> SO <sub>4</sub> (no liquid phase)	2	25–33	68–42	7.4	<0.3	16.1	34.9	3.4	10.8±0.5
12	H <sup>+</sup> =9.2, NH <sub>4</sub> <sup>+</sup> =6.7, HSO <sub>4</sub> <sup>-</sup> =11.7, SO <sub>4</sub> <sup>2-</sup> =2.1	0.5	25–33	57–33	11.4	<0.3	17.3	40.4	3.6	10.0±0.3

<sup>a</sup> Initial seed composition was estimated using extended inorganic aerosol thermodynamics model II (E-AIM, <http://www.aim.env.uea.ac.uk/aim/aim.php>). <sup>b</sup> Ratios for ammonium sulfate/sulfuric acid aqueous solution. <sup>c</sup> Initial and final temperature and RH are reported.



550 **Table 2. Comparison of experimental parameters and SOA yields reported in literature for the photooxidation of  $\alpha$ -pinene.**

Reference	Temp. (°C)	RH (%)	Oxidant	Seed	NO <sub>x</sub> (ppb)	$\alpha$ -pinene (ppb)	$\Delta$ HC ( $\mu\text{g m}^{-3}$ )	$\Delta M_0$ ( $\mu\text{g m}^{-3}$ )	SOA Yield (%)
Chu et al. (2014)	28	12, 50	HONO	AS	n.a.	8.1, 11.7	n.a.	5.9, 9.3	15.1, 23.4
	28	12,50	HONO	FeSO <sub>4</sub>	n.a.	9.7, 10.0	n.a.	5.0, 2.9	10.9, 5.7
Kim and Paulson (2013)	33–42 <sup>a</sup>	15–25 <sup>a</sup>	propene	no seed	47–230	143–153	n.a.	9–118	5.9–17
Eddingsaas et al. (2012)	20–25	<10	H <sub>2</sub> O <sub>2</sub>	AS	n.a.	45.0–48.5	247–265	63.5–76.6	25.7–28.9
	20–23	<10	HONO, CH <sub>3</sub> ONO	AS	~800	44.9–52.4	249–258	37.2–60.3	14.4–24.2
Ng et al. (2007a)	23–25	5.3–6.4	H <sub>2</sub> O <sub>2</sub>	AS	0,1	n.a.	76.7, 264.1	29.3, 121.3	37.9–45.8
	25–26	3.3–3.7	H <sub>2</sub> O <sub>2</sub> +NO, HONO	AS	198–968	n.a.	69.8–259.1	4.5–40.8	6.6–21.2
Kleindienst et al. (2006)	26.3	29	NO <sub>x</sub>	no seed	242, 543	2550	1190, 815	130, 67.3 <sup>b</sup>	10.9, 8.3 <sup>c</sup>
	26.3	29	NO <sub>x</sub>	sulfate	242, 543	2550	1190, 815	87–172 <sup>b</sup>	10.7–14.5 <sup>c</sup>
Takekawa et al. (2003)	10	~60	propene	Na <sub>2</sub> SO <sub>4</sub>	30–53	55–100	260–540	36–89	20–23
	30	~60	propene	Na <sub>2</sub> SO <sub>4</sub>	54–102	93–196	500–1000	20–95	5.2–10
Odum et al. (1996)	35–40	~10	propene	AS	300	~19–143	104–769	1.3–96.0	1.25–12.5

<sup>a</sup> Final temperature and RH were presented. <sup>b</sup> OC mass was reported. <sup>c</sup> SOC yield was reported.



## Figures

555

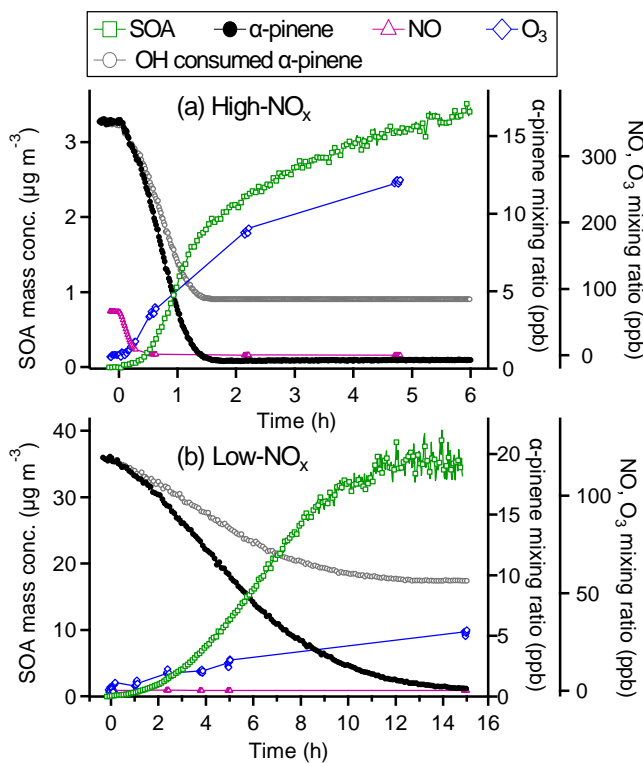
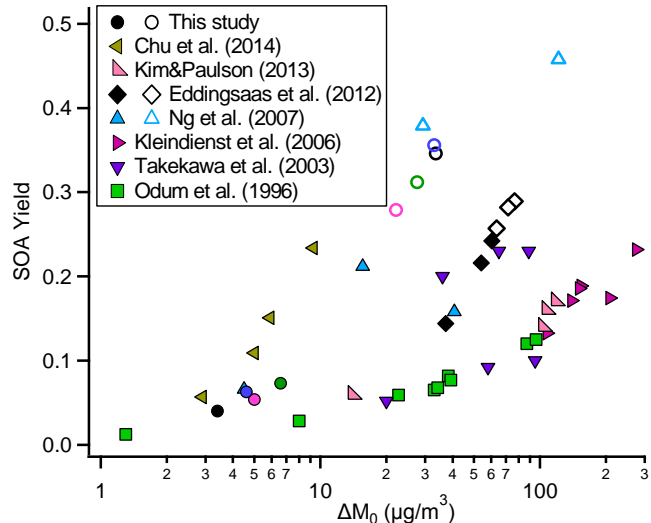


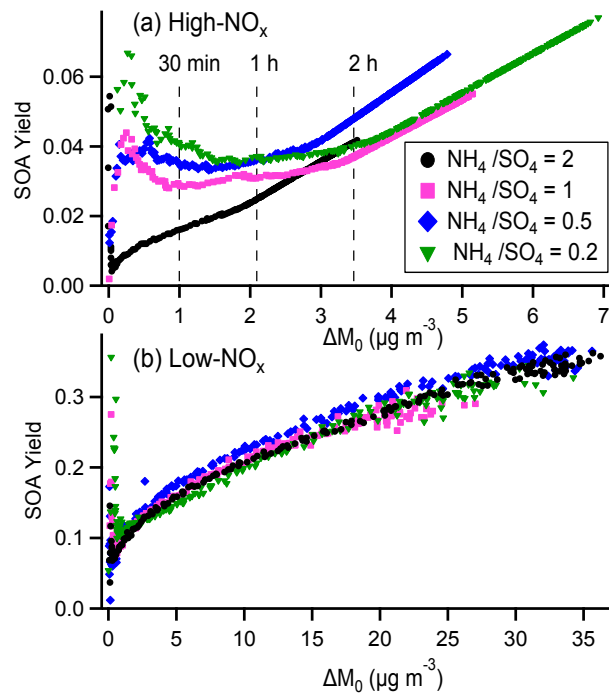
Figure 1. Time series of the mass concentrations of generated SOA and the mixing ratios of NO,  $\text{O}_3$ , total  $\alpha$ -pinene decay, and OH consumed  $\alpha$ -pinene in (a) high- and (b) low- $\text{NO}_x$  experiments using ammonium sulfate as seed particles. Time = 0 hour is defined as  $\alpha$ -pinene photooxidation initiated when the lamps were turned on.



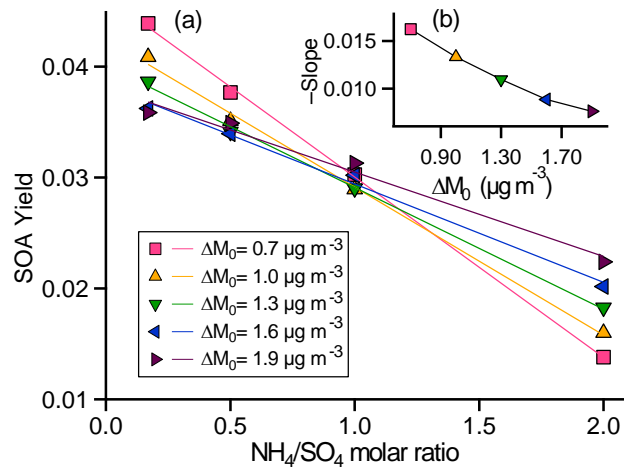
560

Figure 2. Comparison of final  $\alpha$ -pinene SOA yields as a function of organic mass concentration ( $\Delta M_0$ ) under high- and low- $\text{NO}_x$  conditions in this study with those reported previously. The solid and open symbols represent the SOA yields under high- and low- $\text{NO}_x$  conditions, respectively. The black, pink, blue, and green cycles represent the SOA yield for experiments in this study with  $\text{NH}_4/\text{SO}_4$  molar ratios of 2, 1, 0.5, and 0.2, respectively. A factor of 1.6 was used to convert SOC yield and OC mass concentration to SOA yield and OA mass concentration in Kleindienst et al. (2006).

565

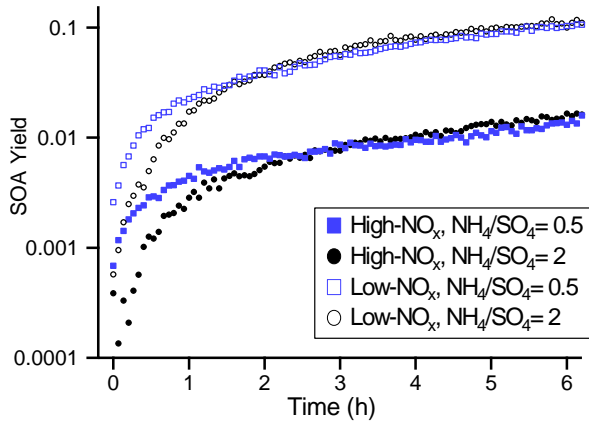


**Figure 3. SOA yields as a function of organic mass concentrations for experiments using seed particles with varied acidity levels under (a) high- and (b) low- $\text{NO}_x$  conditions. The dashed lines in (a) represent the irradiation time at approximately 30 min, 1 hour, and 2 hours, respectively.**



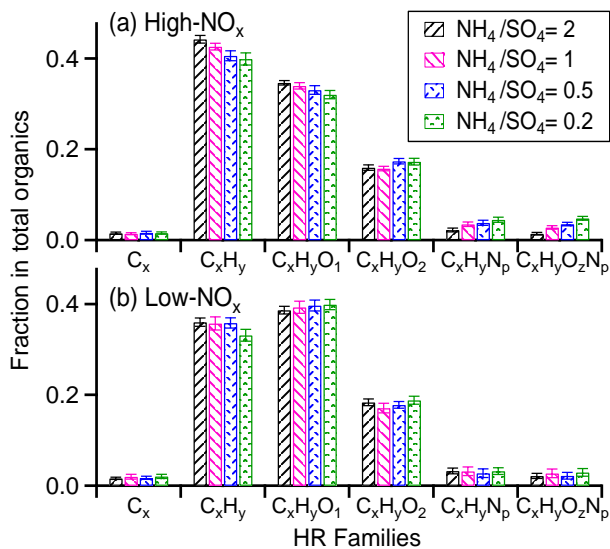
570

**Figure 4.** (a) SOA yield versus  $\text{NH}_4/\text{SO}_4$  molar ratio in the initial period of photooxidation (approximately 0–1 hours) under high- $\text{NO}_x$  conditions. The colored lines represent the linear fitting of the markers. The SOA yields at specific  $\Delta M_0$  values were retrieved from the plotting of SOA yields versus  $\Delta M_0$  in Figure 3a. (b) The slope derived from the fitting of SOA yields with  $\text{NH}_4/\text{SO}_4$  molar ratios in (a) increased with  $\Delta M_0$ .



575

**Figure 5.** The increase of SOA yields with time for experiments with injecting neutral and acidic seed particles after  $\alpha$ -pinene photooxidation for 2 and 4 hours under high- and low- $\text{NO}_x$  conditions, respectively (Exp. 9–12 in Table 1). Time = 0 hour represents the beginning of reactive uptake of oxidation products after seed particles added.



580 **Figure 6.** The mass fractions of organic fragment groups in total organic aerosols under (a) high- and (b) low- $\text{NO}_x$  conditions. The organic mass spectra were averaged for the irradiation times of 1–6 and 2–12 hours under high- and low- $\text{NO}_x$  conditions, respectively. The bars represent the standard deviations ( $\pm 1\sigma$ ) of the mean values for individual fragment groups.

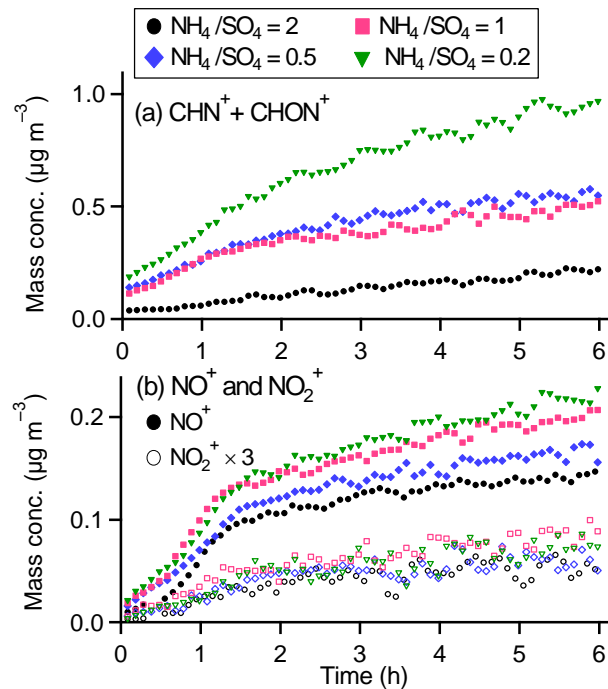


Figure 7. The temporal variations of (a) total N-containing organic fragments (the sum of  $\text{C}_x\text{H}_y\text{N}_z^+$  and  $\text{C}_x\text{H}_y\text{O}_z\text{N}_p^+$ ) and (b)  $\text{NO}^+$  and  $\text{NO}_2^+$  fragments for experiments using neutral and acidic particles under high- $\text{NO}_x$  conditions.

585